

## Nonlinear dependence of set time on pulse voltage caused by thermal accelerated breakdown in the Ti/HfO<sub>2</sub>/Pt resistive switching devices

M. G. Cao, Y. S. Chen, J. R. Sun, D. S. Shang, L. F. Liu et al.

Citation: *Appl. Phys. Lett.* **101**, 203502 (2012); doi: 10.1063/1.4766737

View online: <http://dx.doi.org/10.1063/1.4766737>

View Table of Contents: <http://apl.aip.org/resource/1/APPLAB/v101/i20>

Published by the [American Institute of Physics](http://www.aip.org).

### Related Articles

Spin filter and molecular switch based on bowtie-shaped graphene nanoflake  
*J. Appl. Phys.* **112**, 104328 (2012)

Reconfigurable liquid metal circuits by Laplace pressure shaping  
*Appl. Phys. Lett.* **101**, 174102 (2012)

Features of temperature dependence of contact resistivity in ohmic contacts on lapped n-Si  
*J. Appl. Phys.* **112**, 063703 (2012)

Ordered ZnO nanorods-based heterojunction light-emitting diodes with graphene current spreading layer  
*Appl. Phys. Lett.* **101**, 121104 (2012)

Realization of ohmic-like contact between ferromagnet and rubrene single crystal  
*Appl. Phys. Lett.* **101**, 073501 (2012)

### Additional information on *Appl. Phys. Lett.*

Journal Homepage: <http://apl.aip.org/>

Journal Information: [http://apl.aip.org/about/about\\_the\\_journal](http://apl.aip.org/about/about_the_journal)

Top downloads: [http://apl.aip.org/features/most\\_downloaded](http://apl.aip.org/features/most_downloaded)

Information for Authors: <http://apl.aip.org/authors>

## ADVERTISEMENT

**AIP** | Applied Physics  
Letters

**EXPLORE WHAT'S NEW IN APL**

**SUBMIT YOUR PAPER NOW!**

**SURFACES AND INTERFACES**  
Focusing on physical, chemical, biological, structural, optical, magnetic and electrical properties of surfaces and interfaces, and more...

**ENERGY CONVERSION AND STORAGE**  
Focusing on all aspects of static and dynamic energy conversion, energy storage, photovoltaics, solar fuels, batteries, capacitors, thermoelectrics, and more...

## Nonlinear dependence of set time on pulse voltage caused by thermal accelerated breakdown in the Ti/HfO<sub>2</sub>/Pt resistive switching devices

M. G. Cao,<sup>1</sup> Y. S. Chen,<sup>1,a)</sup> J. R. Sun,<sup>1,b)</sup> D. S. Shang,<sup>1</sup> L. F. Liu,<sup>2</sup> J. F. Kang,<sup>2</sup> and B. G. Shen<sup>1</sup>

<sup>1</sup>Beijing National Laboratory for Condensed Matter Physics and Institute of Physics, Chinese Academy of Science, Beijing 100190, China

<sup>2</sup>Institute of Microelectronics, Peking University, Beijing 100871, China

(Received 4 October 2012; accepted 25 October 2012; published online 13 November 2012)

Dynamic processes of resistance switching have been systemically investigated for the Ti/HfO<sub>2</sub>/Pt bipolar devices. Different transient characteristics were observed in the set and reset processes. The set process consisted of a waiting step and a following abrupt transition, whereas the reset process demonstrated a gradual resistance change. Nonlinear dependence of set time on pulse voltage was observed and explained by the thermally accelerated dielectric breakdown of local switching regions. The accumulation and dissipation effects observed for different pulse treatments strongly supported the proposed model, which suggests a possible approach to overcome the voltage-time dilemma. © 2012 American Institute of Physics. [<http://dx.doi.org/10.1063/1.4766737>]

In recent years, interests in the effect of electric field-triggered resistance switching (RS) have remarkably increased due to the potential application for next generation non-volatile memory, namely resistive random access memory (RRAM).<sup>1–3</sup> The RS effect was observed in most dielectric oxides, including binary oxides, perovskite oxides, and oxide-based heterojunctions.<sup>4–9</sup> Generally, the simple sandwich structure, an oxide insulating layer inserted between a top and a bottom electrode (TE and BE), was adopted in RRAM devices. It is generally believed that the formation and disruption of conductive filaments (CFs) in the insulating layer are responsible, respectively, for the low resistance state (LRS) and high resistance state (HRS) transitions of the device.<sup>10,11</sup> However, the physical origins of CFs vary from device to device, which results in complicated switching characteristics. According to its dependence on electric polarity, the RS effect can be classified as two categories: unipolar and bipolar switching. Usually, the CFs in unipolar devices are originated from the change of material stoichiometry caused by local Joule heating.<sup>12,13</sup> In contrast, the ion movement driven by electric field is dominant for bipolar switching. According to the type of migrated ions, the bipolar devices can be further divided into electrochemical metallization memory devices and valence change memory devices.<sup>10,14,15</sup> In the former devices, the CFs are consisted of active metal cations such as Ag<sup>+</sup> and Cu<sup>+</sup>, whereas they are formed by oxygen vacancies (V<sub>os</sub>) in the later ones.

Although the RS behavior has been intensively investigated, most of the previous works were focused on static performances such as uniformity, reliability, retention, and the dynamic process of the RS was less concerned. As demonstrated by the following researches, the dynamic process study may reveal some inherent properties of the RRAM devices from an alternative perspective.<sup>16</sup> Recently, Lee *et al.* reported a switching speed as high as sub-nanosecond

for HfO<sub>x</sub>-based device.<sup>17</sup> In this kind of devices, oxygen vacancies generated by dielectric breakdown have been believed to be the mobile defects in the CFs. It is astonishing that the oxygen vacancy motion can be raised up to a so high speed. Meanwhile, Waser *et al.* found that the fast switching speed and long retention time, both of which are required by practical application, always conflicted with each other for the RRAM devices.<sup>10</sup> This is called as “voltage-time dilemma,” and is closely related to the distinctive features of the ion generation/recombination and motion under electric field. It is obvious that a thorough research on the dynamic process of RS may lead to a deep understanding of these phenomena, especially how the CFs form and rupture under electric fields. Based on this consideration, in this Letter, we performed a systematic study on the switching dynamics of the Ti/HfO<sub>2</sub>/Pt bipolar devices. We found that the set process consisted of a waiting step and an abrupt resistance drop, whereas the reset process demonstrated the gradual resistance change. Thermally accelerated breakdown of local switching regions was suggested regarding the nonlinear dependence of set time on pulse voltage, which was further proved by the accumulation and dissipation effects for different pulse treatments.

Ti/HfO<sub>2</sub>/Pt devices (Fig. 1(a)) were fabricated following the procedures below: About 30 nm metal Hf layer was first deposited on Pt/Ti/SiO<sub>2</sub>-coated silicon substrates by reactive sputtering, and then *in situ* annealed at 600 °C in O<sub>2</sub> to form HfO<sub>2</sub>. After that, a 100 nm Ti layer was deposited and patterned into squares of the dimension of 0.1 × 0.1 mm<sup>2</sup>. In electrical measurements, the voltage bias was applied to Ti (TE), and Pt (BE) was grounded. To trigger the RS effect, a forming voltage of +15 V was applied to the as-prepared device in advance. Typical bipolar switching behavior was observed for the followed DC sweeps of 0→2 V→0→−2 V→0: The device first undergoes a HRS-to-LRS transition at a critical voltage of  $V_{set}$ , as indicated by the current jump to compliance value (0.5 mA), and then remains in the LRS for subsequent sweeps until a slow transition back to the HRS

<sup>a)</sup>Email: yschen@aphy.iphy.ac.cn.

<sup>b)</sup>Email: jrsun@iphy.ac.cn.

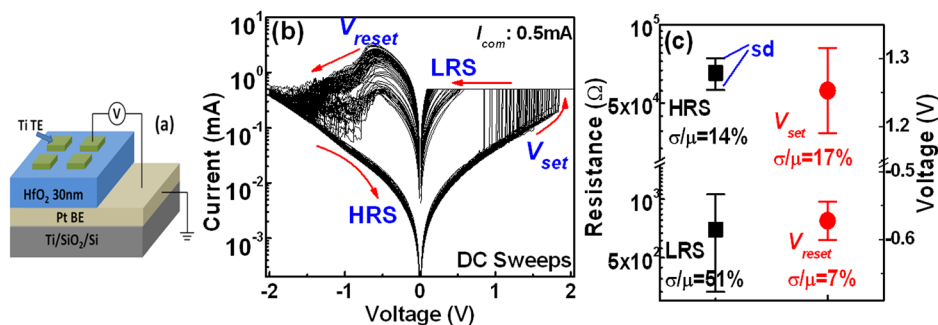


FIG. 1. (a) Schematic structure of the Ti/HfO<sub>2</sub>/Pt device. (b) Typical bipolar RS behavior of the Ti/HfO<sub>2</sub>/Pt device switched by DC voltage sweeps. (c) The parameter statistics of 100 switching cycles, including HRS, LRS,  $V_{set}$ , and  $V_{reset}$ . The solid point is the mean value, and the error bar represents the standard deviation.

when the DC bias sweeps through the reset voltage ( $V_{reset}$ ) (Fig. 1(b)). The bistable switching is well repeatable for hundreds of cycles. As demonstrated by the  $I$ - $V$  loops and the distributions of resistances and switching voltages shown in Fig. 1(c), the variance is much smaller in the reset process than in the set process. The HRS/LRS switching ratio is in the order of  $10^2$  and slightly decays after  $10^4$  cycles. The good uniformity and sustained endurance give us an opportunity to further investigate the dynamics process in the HfO<sub>2</sub> devices.

The experiment setup for dynamic process study is schematically shown in the inset diagram in Fig. 2(a). When the pulse signal is applied to the circuit, a two channel oscilloscope would synchronously capture the output voltage (CH1,  $V_{app}$ ) and the transient current, by measuring the voltage drop on a standard resistor (100 Ω) connected in series to the

device (CH2,  $V_{R0}$ ). Figure 2(a) illustrates the switching response of the device in a full set-reset cycle triggered by  $\pm 3$  V pulses. It clearly demonstrates the different switching dynamics for the two processes. The set process consists of two distinct steps. When positive pulse is applied, the current first keeps at a low level for a while, and then steeply jumps to a high level. It means that the device will wait for a finite period of time ( $T_{wait}$ ) before the HRS-to-LRS transition. The abrupt jump occurs very quickly, finishing in 20 ~ 30 ns. It is mostly limited by the response time of the circuit. Therefore, the total set time is mainly determined by  $T_{wait}$ . Fig. 2(b) shows the current responses in three set processes of the same device. The  $T_{wait}$  varies from cycle to cycle, distributing in a wide range. Meanwhile, the resistance of the LRS is also significantly scattered. These results reflect the intrinsic randomness of the dielectric breakdown. Different from the

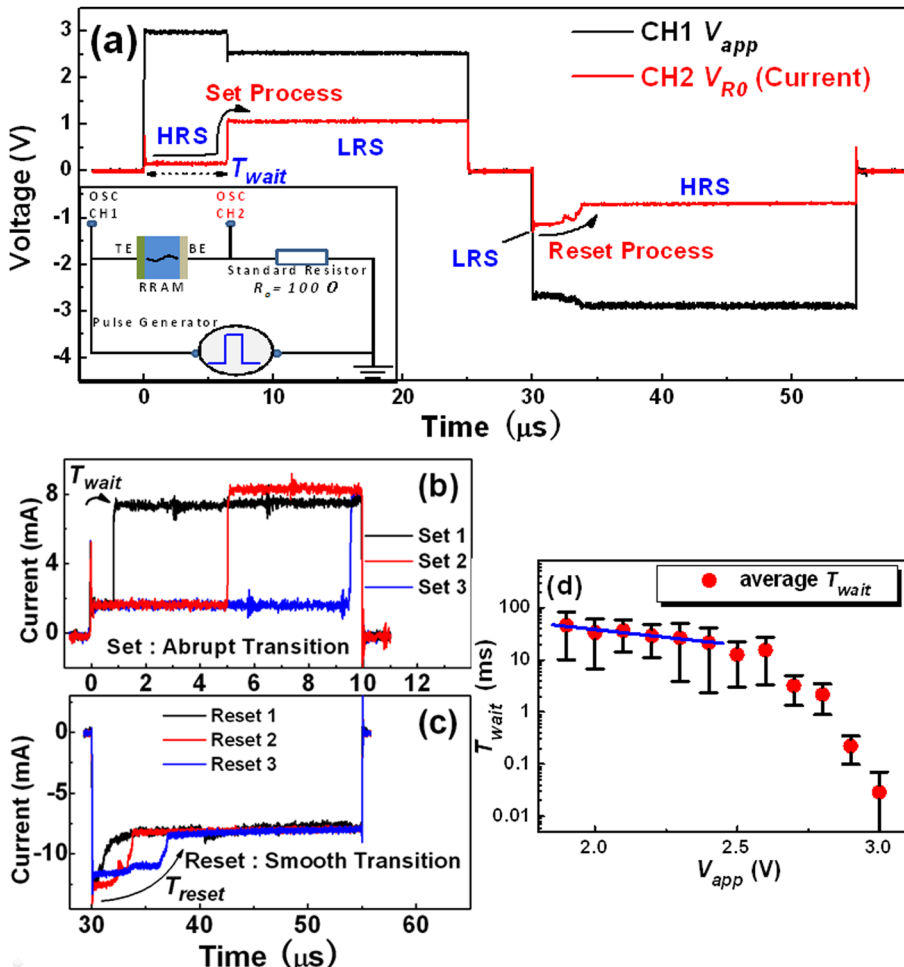


FIG. 2. (a) The switching dynamics of set/reset processes of the device triggered by  $\pm 3$  V square pulses. Inset is the measuring circuit. (b) The fluctuations of the transient characteristics recorded in three of set or reset (c) processes. (d) The nonlinear  $T_{wait}$ - $V_{app}$  dependence. The  $\ln T_{wait}$  is linearly reduced with  $V_{app}$  at the lower voltage region. And a sharp decline in  $T_{wait}$  of three orders of magnitude is observed in the higher voltage region.

set process, the reset process is much smoother. The current responses instantaneously to the pulse signal, without the waiting stage to the resolution of 20 ns (the rising edge of voltage pulse), and the device gradually switches back to the HRS in a few microseconds (see Fig. 2(c)). Similar to the case of DC sweeps, the pulse-induced reset process also demonstrates reduced fluctuation compared to the set process.

To get further information on the two-step set process, we have measured the transient characteristics under different set pulses. The device was switched to the LRS by the positive pulse with the amplitude between 1.9 V and 3 V, and then to the HRS by a negative pulse of  $-3$  V. The reset pulse was fixed to a constant value to ensure the comparability of the starting state for each cycling. Although the  $T_{\text{wait}}$  disperses in a wide range, its mean value, obtained by averaging over tens of switching cycles, shows a monotonically decrease with the increased amplitude of applied pulse. Furthermore, the  $T_{\text{wait}}-V_{\text{app}}$  relation is different in the low and high voltage regions. As shown in Fig. 2(d),  $\ln T_{\text{wait}}$  shows first a linear decrease with the increase of  $V_{\text{app}}$  from  $\sim 49$  ms at 1.9 V to  $\sim 21$  ms at 2.4 V, and then a rapid drop from  $\sim 20$  ms to  $\sim 20$   $\mu$ s when  $V_{\text{app}}$  further increases from 2.5 V to 3.0 V. It is worth to indicate that, although the device resistance is almost invariant for  $t < T_{\text{wait}}$ , the definite  $T_{\text{wait}}-V_{\text{app}}$  dependence suggests the occurrence of some changes in sample state in the waiting period. The fact that a low/high  $V_{\text{app}}$  needs a long/short waiting time may imply an accumulation of the state change before the abrupt resistance drop.

To answer the question what kind of physical effect has been accumulated in the waiting stage and whether the

accumulated effect would be dissipated after removing electric field, contrast experiments were performed using different pulse trains to trigger the set process. For case one, a single pulse with an amplitude of 2.3 V and a width longer than  $T_{\text{wait}}$  was applied to the device in the HRS, and the corresponding  $T_{\text{wait}}$  was recorded (Fig. 3(a)). For case two, the device was set by a series of short pulses (2.3 V in amplitude and 1  $\mu$ s in width) with different separations, and the  $T_{\text{wait}}$  was defined as the total time for the device under field stress before the HRS-LRS transition. As an example, in Fig. 4(b), we show a typical set process triggered by successive pulses. The device keeps in the HRS in the first six pulses and abruptly jumps to the LRS in pulse 7. In this case, the  $T_{\text{wait}}$  is  $6 \mu\text{s} + 0.15 \mu\text{s}$ , where  $0.15 \mu\text{s}$  is the waiting time in pulse 7 (Fig. 4(c)). After each set operation, a  $-3$  V pulse was applied to drive the device back to the HRS for the next cycling. This procedure was repeated tens of times to get the averaged  $T_{\text{wait}}$ . Fascinatingly, we found that the  $T_{\text{wait}}$  would increase with the space time (Fig. 3(d)). This feature was observed in all studied samples, and here we show two typical results. For device 1,  $T_{\text{wait}}$  increases from  $8.0 \mu\text{s}$  to  $11.2 \mu\text{s}$  and  $19.1 \mu\text{s}$  as the space time grows from 0 (corresponding to the single pulse) to 1  $\mu\text{s}$  and 5  $\mu\text{s}$ . Similarly, the  $T_{\text{wait}}$  of device 2 increases from  $1.7 \mu\text{s}$  to  $2.1 \mu\text{s}$  and  $4.3 \mu\text{s}$  for the corresponding growth of pulse space. These results give us a sensation that the state change caused by pulse stress is weakened by the time space between two neighboring pulses. In other words, the effect of the pulse stress can be accumulated, whereas the pulse space leads to a dissipation of such effect. It implies that some intrinsic properties of the switching layer, other than resistance, are changed

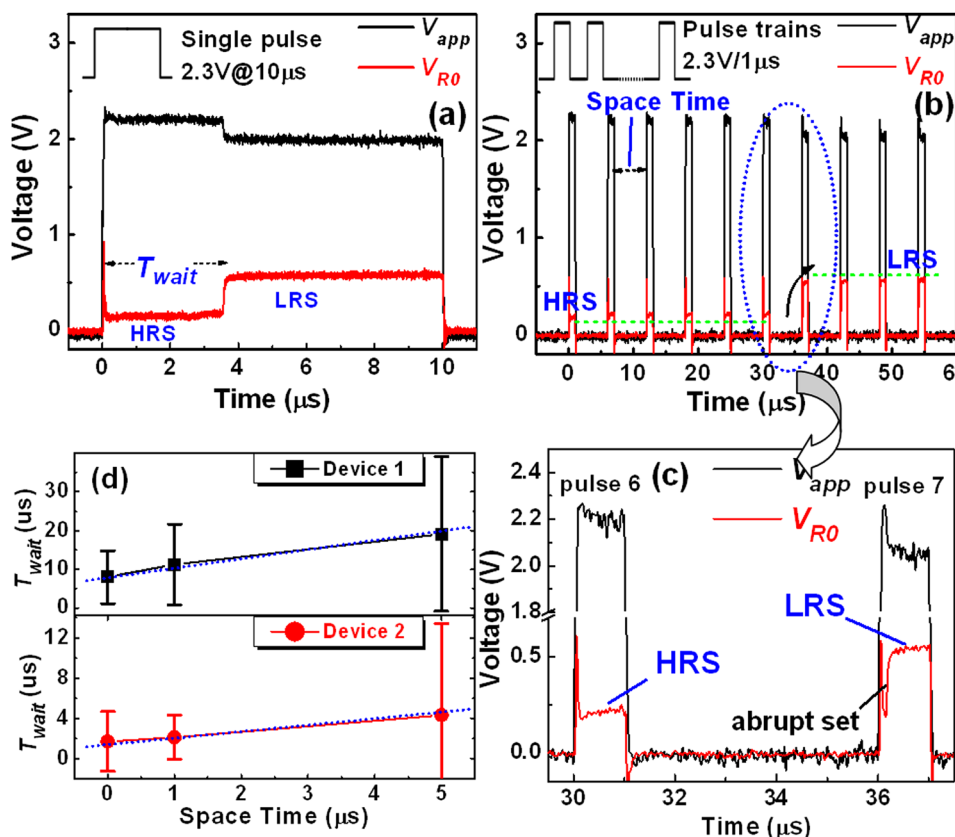


FIG. 3. (a) The dynamics process of the device set by a single pulse. (b) The dynamics process of the device set by a series of 1  $\mu$ s pulses and (c) the enlarged drawing of the transient current in pulse 7. (d) The dependence of  $T_{\text{wait}}$  on the space time for two devices. The average  $T_{\text{wait}}$  and fluctuation are both increased with the space time.

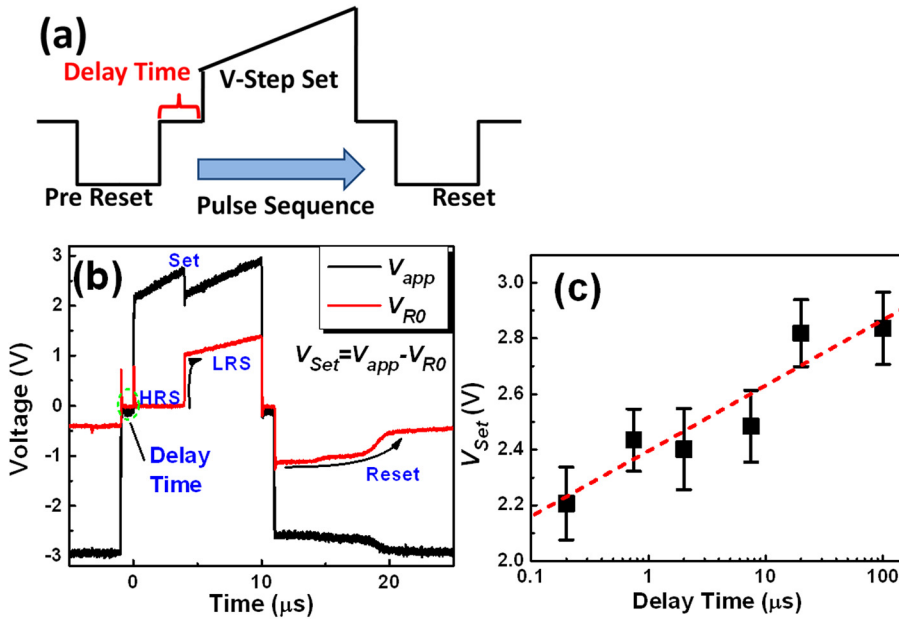


FIG. 4. (a) Schematic of the pulse train sequence, consisting of a pre-reset pulse, a trapezoidal set pulse, and a reset pulse. (b) The dynamic process of the device switched by the above pulse sequence. (c) The  $V_{Set}$  demonstrates a logarithmic increase on the delay time, from about 2.2 V with 200 ns delay to about 2.8 V with 100  $\mu\text{s}$  delay.

during the waiting stage, and it is this change that facilitates the following dielectric breakdown. Thus, the increase of  $T_{wait}$  with the space time can be understood.

The above experiments explore the effect of space time between two neighboring positive pulses. It is further found that the space between a pre-reset negative pulse and the following set pulse can also influence the dielectric breakdown. To avoid the wide distribution of  $T_{wait}$  under square set pulses, here, trapezoidal set pulses are used for the convenience of measurements. Fig. 4(a) is a sketch of the pulse sequence, consisting of a pre-reset pulse of  $-3$  V, a trapezoidal set pulse ramped from 2.2 V to 3 V in 10  $\mu\text{s}$ , and a reset pulse of  $-3$  V. Similar to the phenomena observed under square pulses, as shown in Fig. 4(b), the device keeps in the HRS when  $V_{app}$  is low and abruptly jumps to the LRS when  $V_{app}$  reaches a threshold value. In this case, the set voltage  $V_{set}$  can be calculated as  $V_{set} = V_{app} - V_{R0}$ . It may be instructive to inspect the correlation between the decay time, the time interval of pre-reset pulse and set pulse, and the  $V_{set}$ . Interestingly,  $V_{set}$  shows a remarkable increase with the decay time, growing from 2.21 V to 2.83 V as the decay time varies from 0.2  $\mu\text{s}$  to 100  $\mu\text{s}$  (Fig. 5(c)). In the case of square set pulse, the accumulation effect of pulse stress is measured by  $T_{wait}$ , and a stronger accumulation leads to a shorter  $T_{wait}$ . In the case of trapezoidal set pulse, the accumulation effect is reflected by  $V_{set}$ , and a lower  $V_{set}$  means an easier dielectric breakdown. The increased decay time causes a growth of  $V_{set}$ , which means a dissipation of the effect of the pre-reset pulse in the decay time. This result indicates that the accumulation effect of pulse stress on the HRS is independent of electrical polarity.

Since the effect of space time between two neighboring pulses occurs under either positive or negative pulses and a long space time always makes the dielectric breakdown difficult, the space time effect may be thermally originated. It is possible that thermal energy is accumulated during field stressing. The waiting time could be a measure of the time required by accumulating enough thermal energy to get a dielectric breakdown. However, the space time between

pulses produces an opposite effect by dissipating the accumulated energy, and therefore leads to a growth in  $T_{wait}$ . To explain the nonlinear  $T_{wait}-V_{app}$  dependence, a model of thermally accelerated breakdown of the local switching region was proposed. Based on the Arrhenius law, the  $T_{wait}$  can be described as

$$T_{wait} \propto \frac{1}{f} \exp\left(\frac{E_a - \alpha \cdot E}{k_B \cdot T_e}\right),$$

where  $f$  is attempt frequency,  $E_a$  is activation energy,  $E$  is the electric field in the switching layer,  $\alpha$  is the field acceleration parameter, and  $T_e$  is the effective temperature. According to this equation,  $\ln T_{wait}$  will vary linearly with applied field when other parameters are constants. This prediction tallies with the  $T_{wait}-V_{app}$  relation in the low bias region shown in Fig. 2(d). Based on a simple double-well model, the activation energy of oxygen ions is linearly lowered by the applied field as  $E'_a = E_a - \alpha E = E_a - 2e \cdot \frac{d}{2} \cdot \frac{V_{app}}{L}$ , where  $d$  is the lattice constant of  $\text{HfO}_2$  and  $L$  is the effective thickness of the switching layer. From the intercept and slope of the fitting curve ( $\ln T_{wait} = -0.583 - 1.34146 V_{app}$ ), we can deduce that  $E_a$  is  $\sim 0.8$  eV and  $L$  is  $\sim 10$  nm (assuming  $f = 10^{13}$  Hz,  $T_e = 300$  K, and  $d = 3.5$   $\text{\AA}$ ). It is a reasonable assumption that  $T_e$  may be raised well above the room temperature by the Joule heating in the local switching region.<sup>18,19</sup> Generally, the  $T_e$  can be approximated by  $T_e = T_0 + V_{app}^2 \cdot \frac{R_{th}}{R}$ , where  $T_0$  is the reference temperature,  $R_{th}$  is the equivalent thermal resistance, and  $R$  is the resistance.<sup>18</sup> In that case, a temperature-modified attempt frequency,  $f = f_0 \cdot \left(\frac{T_e}{T_0}\right)^n$ , should be considered ( $0 < n < 1$ ). It is obvious that an increase in  $T_e$  will cause a reduction in both the  $\frac{1}{f}$  term and the exponential term, leading to a rapid drop of  $T_{wait}$ . This analysis implies that the deviation from linearity of the  $\ln T_{wait}-V_{app}$  relation in high  $V_{app}$  region could be a consequence of enhanced Joule heating. According to the expression of  $T_e$ , a large  $\frac{R_{th}}{R}$  factor will enhance the thermal effect, thus speed up the RS. Recently, Menzel *et al.*<sup>20</sup> reported a temperature-accelerated drift of oxygen vacancies in the

SrTiO<sub>3</sub> material. All these results give us an inspiration to trigger the HRS-LRS transition with the help of local Joule heating, which favors a fast switching speed and maintains a good retention at very low read voltage. It may be a possible way to overcome the “voltage-time dilemma.”

In summary, the switching dynamics of the Ti/HfO<sub>2</sub>/Pt bipolar devices were systematically investigated. The different transient characteristics of “abrupt” set and “gradual” reset processes were demonstrated. The thermally accelerated breakdown was proposed to explain the nonlinear  $T_{wait}-V_{app}$  dependence in set process, which was confirmed by the accumulation and dissipation phenomena in different pulse trains. Further studies are in progress to get a thorough understanding of the correlations between thermal and electric effect in the RS phenomena.

This work has been supported by the National Basic Research of China, the National Natural Science Foundation of China, the Knowledge Innovation Project of the Chinese Academy of Sciences, and the Beijing Municipal Natural Science Foundation.

<sup>1</sup>K. Szot, W. Speier, G. Bihlmayer, and R. Waser, *Nature Mater.* **5**, 312 (2006).

<sup>2</sup>R. Waser and M. Aono, *Nature Mater.* **6**, 833 (2007).

<sup>3</sup>A. Sawa, *Mater. Today* **11**, 28 (2008).

<sup>4</sup>S. B. Lee, S. C. Chae, S. H. Chang, J. S. Lee, S. Seo, B. Kahng, and T. W. Noh, *Appl. Phys. Lett.* **93**, 212105 (2008).

<sup>5</sup>D. Choi, D. Lee, H. Sim, M. Chang, and H. Hwang, *Appl. Phys. Lett.* **88**, 082904 (2006).

<sup>6</sup>J. J. Yang, M. D. Pickett, X. Li, D. A. A. Ohlberg, D. R. Stewart, and R. S. Williams, *Nat. Nanotechnol.* **3**, 429 (2008).

<sup>7</sup>S. Q. Liu, N. J. Wu, and A. Ignatiev, *Appl. Phys. Lett.* **76**, 2749 (2000).

<sup>8</sup>A. Beck, J. G. Bednorz, Ch. Gerber, C. Rossel, and D. Widmer, *Appl. Phys. Lett.* **77**, 139 (2000).

<sup>9</sup>Y. S. Chen, L. P. Chen, G. J. Lian, and G. C. Xiong, *J. Appl. Phys.* **106**, 023708 (2009).

<sup>10</sup>R. Waser, R. Dittmann, G. Staikov, and K. Szot, *Adv. Mater.* **21**, 2632 (2009).

<sup>11</sup>D. H. Kwon, K. M. Kim, J. H. Jang, J. M. Jeon, M. H. Lee, G. H. Kim, X. S. Li, G. S. Park, B. Lee, S. Han, M. Kim, and C. S. Hwang, *Nat. Nanotechnol.* **5**, 148 (2010).

<sup>12</sup>D. Ielmini, C. Cagli, and F. Nardi, *Appl. Phys. Lett.* **94**, 063511 (2009).

<sup>13</sup>S. H. Chang, J. S. Lee, S. C. Chae, S. B. Lee, C. Liu, B. Kahng, D. W. Kim, and T. W. Noh, *Phys. Rev. Lett.* **102**, 026801 (2009).

<sup>14</sup>X. Guo, C. Schindler, S. Menzel, and R. Waser, *Appl. Phys. Lett.* **91**, 133513 (2007).

<sup>15</sup>A. Baikalov, Y. Q. Wang, B. Shen, B. Lorenz, S. Tsui, Y. Y. Sun, Y. Y. Xue, C. W. Chu, *Appl. Phys. Lett.* **83**, 957 (2003).

<sup>16</sup>S. B. Lee, H. K. Yoo, S. H. Chang, L. G. Gao, B. S. Kang, M.-J. Lee, C. J. Kim, and T. W. Noh, *Appl. Phys. Lett.* **98**, 053503 (2011).

<sup>17</sup>H. Y. Lee, Y. S. Chen, P. S. Chen, P. Y. Gu, Y. Y. Hsu, S. M. Wang, W. H. Liu, C. H. Tsai, S. S. Sheu, P. C. Chiang, W. P. Lin, C. H. Lin, W. S. Chen, F. T. Chen, C. H. Lien, and M.-J. Tsai, *Tech. Dig. IEDM.* **2010**, 460.

<sup>18</sup>U. Russo, D. Ielmini, C. Cagli, and A. L. Lacaita, *IEEE Trans. Electron Devices* **56**, 186 (2009).

<sup>19</sup>S. M. Yu and H.-S. Philip Wong, *IEEE Electron Device Lett.* **31**, 1455 (2010).

<sup>20</sup>S. Menzel, M. Waters, A. Marchewka, U. Böttger, R. Dittmann, and R. Waser, *Adv. Funct. Mater.* **21**, 4487 (2011).